Trophic connectivity between offshore upwelling and the inshore food web of Banc d'Arguin (Mauritania): New insights from isotopic analysis

Antoine Carlier, Laurent Chauvaud, Matthijs van Der Geest, François Le Loc'h, Michel Le Duff, Marc Vernet, Jean Raffray, Djibril Diakhaté, Pierre Labrosse, Abdoulaye Wagué, et al.

HAL Id: hal-01167013
https://hal.sorbonne-universite.fr/hal-01167013

Submitted on 23 Jun 2015

Trophic connectivity between offshore upwelling and the inshore food web of Banc d'Arguin (Mauritania): New insights from isotopic analysis

Antoine Carlier[1#*], Laurent Chauvaud[1], Matthijs van der Geest[2,3], François Le Loc'h[1,4], Michel Le Duff[1], Marc Vernet[5], Jean Raffray[1], Djibril Diakhaté[6], Pierre Labrosse[6], Abdoulaye Wagué[6], Clément Le Goff[7], Francis Gohin[7], Bertrand Chapron[8], Jacques Clavier[1]

[*] Corresponding author. Tel: +33-2 98 22 43 91; fax: +33-2 98 22 45 48.

E-mail Address: Antoine.Carlier@ifremer.fr

[#] Current address: IFREMER-Centre Bretagne, DYNECO-Laboratoire d'écologie benthique, 29280 Plouzané, France.

[1] LEMAR, UMR 6539 (CNRS-UBO-IRD-IFREMER), Institut Universitaire Européen de la Mer, Technopôle Brest Iroise, Place Nicolas Copernic, 29280 Plouzané, France.

[2] Department of Marine Ecology, NIOZ Royal Netherlands Institute for Sea Research, P.O. Box 59, 1790 AB Den Burg (Texel), The Netherlands.

[3] Animal Ecology Group, Centre for Ecological and Evolutionary Studies (CEES), University of Groningen, PO Box 11103, 9700 CC Groningen, The Netherlands

[4] Ecosystèmes Marins Exploités, UMR 212 EME (IRD-IFREMER-UMII), Institut de Recherche pour le Développement, Centre de Recherche Halieutique, Avenue Jean Monnet, BP 171 34203, Sète Cedex, France.

[5] CNRS, UPMC Univ. Paris 06, UMR 7144, Adaptation et Diversité en Milieu Marin, Equipe Chimie Marine, Station Biologique de Roscoff, Place Georges Teissier, 29680 Roscoff, France.

[6] IMROP (Institut Mauritanien de Recherche Océanographique et des Pêches), B.P. 22, Nouadhibou, Mauritania.

[7] IFREMER-Centre Bretagne, DYNECO-Laboratoire d'écologie pélagique, 29280 Plouzané, France.

[8] IFREMER-Centre Bretagne, Laboratoire d'Océanographie Spatiale, 29280 Plouzané, France.

ABSTRACT

Banc d'Arguin (BA), Mauritania, is a nationally protected shallow gulf > 10,000 km^2 between the Sahara desert and the upwelling system off the Mauritanian coast. In the southeast, BA consists of a 500 km^2 tidal flat, the most important wintering site for shorebirds using the East Atlantic Flyway. The Mauritanian upwelling-driven phytoplankton production supports the most productive fisheries worldwide, but little is known about its trophic role in the functioning of the inshore BA food web. Using stable isotopes as trophic tracers to distinguish between upwelling-driven phytoplankton, open ocean phytoplankton, and benthic primary producers, we assessed the spatial extent to which the inshore BA food web is fuelled by upwelling-driven phytoplankton production. The $\delta^{13}C$ and $\delta^{15}N$ signals were characterized in dominant primary producers, benthic invertebrate taxa, and various fish species along an offshore–inshore (northwest–southeast) gradient. We also monitored the spatial and temporal extent of upwelling entering BA during 2008 with remote sensing of sea surface temperature and chlorophyll a data. The results suggest that benthic invertebrates and fishes living in the northwestern part of BA depend on the nearby upwelling phytoplankton production, but this food source does not support the intertidal benthic community in southeast BA. Furthermore, the isotopic signatures of fishes suggest weak trophic connectivity between the northern subtidal and southeastern intertidal BA. Our results support the hypothesis that the southeastern tidal flat region functions as a distinct ecosystem with a food web supported mainly by local benthic primary production, which is crucial knowledge for effective management of the pristine BA national park.

Keywords: Banc d'Arguin; West Africa; food web structure; remote sensing; stable isotope; upwelling

1. Introduction

The large Canary Upwelling System (12–43°N) is one of the four major eastern boundary upwelling systems of the world (Arístegui et al., 2006). Within this large marine ecosystem, the Mauritanian sub-region located along the northwest coast of Africa experiences the strongest upwelling events because of persistent and strong northeast trade winds, making it one of the most productive fishing areas worldwide (Minas et al., 1982; Arístegui et al., 2009). Extensive investigations have demonstrated that the Mauritanian continental shelf ecosystem is fuelled primarily by upwelling-enhanced pelagic primary production, resulting in large exploitable stocks of pelagic fish, cephalopods, and shrimp (Josse, 1989; Duineveld et al., 1993; Cury et al., 2000). However, much less work has been focused on the adjacent littoral ecosystem. The food web of this land–ocean interface is likely much more complex than the shelf ecosystem because trophic pathways may be strongly influenced by additional sources of organic matter (e.g., local benthic primary production) that are potentially promoted by nutrient sources (e.g., Sahara dust deposition) other than upwelled nutrient-rich waters.

In this sense, Banc d'Arguin (BA), Mauritania, may help us better understand how offshore-upwelling affects coastal ecosystems. The BA area is characterized by an extensive (10,000 km^2) shallow (< 20 m depth) embayment between the Sahara desert and eastern Atlantic Ocean (Fig. 1). In northwest BA, the Mauritanian upwelling reaches its maximum intensity and is permanent due to the hydrological conditions and topography (Mittelstaedt, 1991; Van Camp et al., 1991). The BA gulf is a transition zone between the northern temperate and southern tropical climates with complex mixing of cold and warm waters originating from the northern Atlantic (Canary current) and the tropics (southern tropical current), respectively (Loktionov, 1993). Therefore, BA represents the geographic boundary limit of many species of temperate and tropical marine flora and fauna. In southeast BA, a

500-km^2 intertidal flat covered mainly by seagrass meadows (Wolff and Smit, 1990) provides and extensive nursery area for many marine species (Jager, 1993; Schaffmeister et al., 2006) and a wintering refuge for over 2 million migratory shorebirds (Altenburg, 1982). The benthic macrofauna of this area is actively exploited by shorebirds and motile marine predators (Wolff et al., 1993b, 2005; Ahmedou Salem et al., 2014). Because of this, approximately 12,000 km^2 of shallow water, tidal flats, and adjacent desert have been included in a marine protected area called the Parc National du Banc d'Arguin (PNBA) since 1976.

The ecological investigations of BA started in the early 1980s with ornithological research (Altenburg et al., 1982; Engelmoer et al., 1984), followed by fisheries surveys by what is now known as the Mauritanian Institute of Oceanographic and Fisheries Research (IMROP). Scientific questions rapidly expanded to the general functioning of the entire gulf, resulting in studies on the influence of upwelling on the tidal flat system in southeast BA. However, apart from an exploration of ecological interactions between the entire BA and the upwelling input (Wolff et al., 1993b), the subtidal food web structure of the gulf is poorly known, mainly because scientific cruises to this area have been hampered by its extreme shallowness and poorly described bottom topography. In addition, the high carrying capacity of the BA tidal flat area for wintering shorebirds is still not fully understood (Wolff et al., 1993a; van der Geest, 2013; Ahmedou Salem et al., 2014).

To better assess organic matter exchange and trophic relationships between the intertidal part of BA and the offshore upwelling area, the connecting subtidal part of BA needs to be investigated. The present study aimed to determine whether the functioning of the subtidal and intertidal BA food web is influenced by the primary production of the Mauritanian upwelling. First, we assessed the extent to which upwelling-driven phytoplankton production supports the inshore BA food web by sampling benthic macrofauna and analyzing it for δ^{13}C and δ^{15}N along a gradient from the subtidal northern BA to the intertidal southeastern BA. In

particular, $\delta^{13}C$ was used as a trophic tracer because it allows us to distinguish between phytoplankton from highly productive regions such as upwelling areas, phytoplankton from the less productive open ocean, and benthic primary producers (Fry and Wainright, 1991). Therefore, by measuring stable isotope ratios in the tissues of primary consumers, we could estimate the trophic influence of the upwelling over a period corresponding to the turnover time of the tissue. Primary consumers were analyzed at the end of spring (i.e., May) based on the assumption that the potential influence of upwelling on the food web would be maximal at that season (Van Camp et al., 1991). These isotopic data were interpreted in the light of remote sensing data for sea surface temperature (SST) and chlorophyll *a* concentrations (Chl *a*) obtained during the same period for the entire Mauritanian coast. These additional data help us to better characterize upwelling activity and subsequent phytoplankton production and to interpret any observed spatial patterns in isotopic signatures of primary consumers collected in our study area.

Second, we aimed to identify the main trophic pathways on which motile consumers (i.e., planktivorous and predatory fish) depend to gain insight into the trophic connectivity between the northern subtidal (presumably more influenced by upwelling) and southern intertidal flat regions of BA. For this purpose, fish caught in distinct areas of BA were characterized isotopically. Fish muscle tissue reflects the diet over a long period of time, which allowed us to create a picture of what fuels the top of the BA food web. Moreover, the isotopic composition of predatory fishes was used as a natural 'tag' to track displacements between isotopically distinct areas.

2. Material and Methods

2.1. Study area

The gulf of BA is located between 19°20' N and 20°30' N along the coast of Mauritania (Fig. 1) and is delineated by Cape Blanc (with rocky shores) to the north and Cape

Timiris (with sandy shores) to the south. With a tidal range of 1.5–2 m, the southeastern part of BA comprises an extensive intertidal flat (500 km^2), 85% of which is covered by dense seagrass (mainly *Zostera noltii*) meadows (Wolff and Smit, 1990). Other seagrass species, such as *Cymodocea nodosa* and *Halodule wrightii,* occur less frequently and are mainly subtidal. The large standing stock of benthic microalgae on the intertidal flats is present mostly on the muddy seagrass-covered areas (Honkoop et al., 2008). On the intertidal *Z. noltii* seagrass beds, the zoobenthos biomass is relatively low but still supports extremely high shorebird densities during the winter (Altenburg et al., 1982; van der Geest, 2013). Wind is likely to be a dominant factor in the functioning of the BA ecosystem, blowing from northerly directions approx. 85% of the time, and high wind speed (> 8 m s^{-1}) occurring from April to June (Dedah, 1993). As a result, the greatest upwelling occurs close to Cape Blanc from March to May (Lathuiliere et al., 2008; Farikou et al., 2013). High macrobenthos biomass and activity rates have been attributed to upwelling during spring in this area (Christensen and Packard, 1977). Therefore, we assumed that the upwelling isotopic signal recorded in the tissues of suspension feeders would be maximal at the end of May.

The gulf exhibits strong seasonal and latitudinal temperature (from 16 to 28°C) and salinity (from 35 to > 38) fluctuations (Dedah, 1993), but both parameters increase along a northwest–southeast gradient. The offshore northwestern zone is affected by upwelling, and then is occupied by cold and less saline waters, while the shallow inshore southeastern zone is occupied by warm and more saline waters due to strong solar radiation and evaporation. BA is characterized by an absence of river inputs, and in most years precipitation is < 30 mm per year (Wolff and Smit, 1990). BA likely has a complex, but poorly characterized, hydrology (Sevrin-Reyssac, 1993) and bathymetry. Investigations in the 1970s indicated a dominant southward flow, with BA acting as a water pump due to the combined actions of the tide and

6

dominant winds (Peters, 1976). However, to our knowledge, no realistic hydrodynamic models have been proposed.

2.2. Sample collection

All samples were collected from May 12–26, 2008, except for microphytobenthos (MPB) and seagrass epiphytes, which were collected from May 8–14, 2008, and on February 1, 2010, respectively. Macrobenthic fauna were sampled at 10 sites that comprise most of the northern subtidal area of BA, from Cape Blanc to the northern entrance of the intertidal flats (close to Iwik village), and from the western shallow sand banks to the coast (Fig. 1; Table 1). Site 1 was chosen as the 'offshore' end of our sampling area because it is located in the permanent and most intensive region of the upwelling. Towards the southeast, we chose sites 9 and 10 as the 'inshore' end of our sampling area, at the northern entrance of the BA intertidal flat area, to investigate the presence of any trophic influence of upwelling on this ecologically important part of BA.

Sampling was performed using the RV *Amrigue* at all subtidal sites (sites 1 to 9) and by hand at low tide at the intertidal site (site 10). Seawater samples were collected at a depth of ~0.5 m using a plastic bottle and pre-filtered through a 100-µm mesh. Suspended particulate organic matter (POM) was recovered on pre-combusted (450°C, 4 h) GF/F 24-mm Whatman filters using a manual pump. POM samples were kept at -20°C.

At sites 1 to 9, benthic invertebrates were collected aboard the RV *Amrigue* using a shell dredge, which was deployed 2–3 times (each for ~20 min) at each sampling site. MPB (mostly the epipelic component) was collected at four seagrass-covered sites and four bare patches at the intertidal flats surrounding the Iwik peninsula (site 10) following a method adapted from the protocol described by Couch (1989) (for more details see Supplement 1). Seagrass leaves were carefully scraped with a scalpel to remove epiphytes, which were

analyzed separately. Epiphytes were resuspended in GFF-filtered seawater, collected on precombusted GF/F filters, and stored frozen at -20°C.

Fish were bought from fishermen on May 22–25, 2008, at three different fishing locations: the economic harbor of Nouadhibou (north of BA) and two Imraguen villages located on the eastern and southeastern sides of BA, Arkeiss and Teichott, respectively (Fig. 1). Fishermen from Nouadhibou use motor pirogues, allowing them to catch fish far from their harbor, but they are not allowed to fish within the PNBA. At Arkeiss and Teichott, fishermen use traditional sailing boats (launches) that prevent them from fishing further than 35 km from their village. Therefore, fish from our three sampling locations originated from distinct fishing areas of BA, with the northward boundary of the Teichott fishing zone at Tidra Island. Targeted fish species represent a large set of feeding behaviors and a wide range of trophic levels, encompassing the whole food web of BA. Care was taken to collect adult specimens of similar size for a given species so that the diet was recorded over as long a period of time as possible. However, collected specimens of the shark *Rhizoprionodon acutus* were juveniles.

2.3 Sample processing

Benthic invertebrates were dissected onboard the RV *Amrigue* (or at Iwik station for samples from site 10), and tissue samples kept at -20°C. Exoskeletons, shells and guts (when possible) were removed using fine forceps. Depending on taxa and body size, whole animals (e.g., polychaetes, bivalves, gastropods), muscle (e.g., crabs, urchins), or small pieces of tissue free of detritus (e.g., sponges) were kept for analysis. For tissues likely to contain carbonates (e.g., calcareous sponges, ophiurids), sub-samples reserved for δ^{13}C analysis were acidified with HCl (10%) until no further effervescence occurred (i.e., < 1 min), while sub-samples reserved for δ^{15}N analysis were left untreated. Dorsal muscles were dissected from the fish and kept at -20°C until processing at the Dakar IRD laboratory. Since lipid content

was low in the analysed invertebrate and fish tissues (C:N ratio always ≤ 4), lipid was not extracted from our samples and $\delta^{13}C$ signal was not lipid-corrected. All samples were freeze-dried and homogenized into a fine powder using a mortar and pestle before isotopic analysis. For POM samples, carbonates were removed by exposing the GF/F filters containing POM to HCl (10%) fumes (4 h). Frozen MPB samples were transported to the Netherlands, freeze-dried at NIOZ, and gently scraped off the GF/F filter into a tin-foil crucible for further stable isotope analysis. Supplement 2 give a detailed description of the method used for stable isotope analysis.

2.4. Remote sensing data

Surface Chl a concentrations were estimated by analyzing satellite images of the whole BA acquired during 2008. Chl a concentration data were derived from the standard remote sensing reflectance of MODIS/Aqua. The MODIS Level-2 reflectance products (reprocessed in 2010, SeaDAS V6.2) were downloaded from the OceanColor/Goddard Space Flight Center WEB. Spatial patterns in Chl a concentration were estimated by applying the Ifremer OC5 algorithm to the spectral remote sensing reflectance (Rrs) of MODIS. This method gives similar results to OC3M/MODIS/NASA in the open ocean but provides more realistic values in turbid waters (Gohin, 2011).

For the entire BA system in 2008, SST was derived daily (at night) from an advanced very high–resolution radiometer (AVHRR), which is a broadband scanner sensing in the visible, near-infrared, and thermal infrared portions of the electromagnetic spectrum. The NOAA/AVHRR has three infrared channels, providing the brightness temperature of the sea surface in three bands: channel 3 (3.6–3.8 µm), channel 4 (10.2–11.2 µm), and channel 5 (11.5–12.5 µm). SST was obtained using a two-channel algorithm: $Ts = T4 + 2 * (T4 - T5) + 0.5$, where T4 and T5 are the brightness temperature of the surface in infrared channels 4 and 5.

2.5. Statistical analysis

Between-site differences in the isotopic values of all suspension-feeding benthic invertebrates were investigated using mean δ^{13}C and mean δ^{15}N values per species per site. This analysis was also performed for the dominant families of suspension-feeders using raw δ^{13}C data pooled per site and for all benthic invertebrate secondary consumers using mean δ^{13}C and mean δ^{15}N values per species per site. Furthermore, we tested for between-site differences in isotopic values for fish caught in three different areas in BA by considering the mean δ^{13}C and mean δ^{15}N values per species per site.

We used parametric tests when both normality (Kolmogorov–Smirnov test) and equal variance (homoscedasticity Lévène test) were observed and non-parametric tests if they were not observed. As parametric tests, we used the t-test and one-way ANOVA (with sampling site as a factor) when comparing isotopic values between two sites or more than two sites, respectively. In addition, we used the Holm–Sidak procedure of pairwise multiple comparison to assess the extent to which isotopic values differed between sites. As non-parametric tests, we used the Mann–Whitney U test and Kruskal–Wallis test to compare isotopic values between two sites or more than two sites, respectively. After the Kruskal–Wallis test, we used the Dunn's procedure of pairwise multiple comparison to assess the extent to which isotopic values between sites differed from each other. We tested for any relationships between the isotopic signals (δ^{13}C, δ^{15}N) of fishes and their individual sizes (mm) using non-parametric Spearman rank correlation. Significant relationships were only found for δ^{13}C of *Umbrina canariensis* (p = 0.007), δ^{15}N of *Pomadasys* spp. (p = 0.008) and δ^{15}N of *Arius* spp. (p = 0.027).

The contribution of upwelling-fuelled POM and inshore POM to the diet of the suspension-feeding benthic invertebrates collected at subtidal sites 1 to 8 was estimated by a

SIAR mixing model (Parnell et al., 2010). The model was run for 500,000 iterations, discarding the first 50,000 iterations. Trophic enrichment values were adapted from literature values obtained with marine bivalves (Dubois et al., 2007; Yokoyama et al., 2005, 2008) and herbivorous marine invertebrates (Vander Zanden and Rasmussen 2001): 3.7 ± 0.9‰ and 0.7 ± 1.2‰ for N and C, respectively. The model was run only with two sources, suspended POM originating from upwelling and suspended POM from inshore waters, as other potential food sources, such as suspended epiphytic algae, macroalgae, and drifting fragments of mangroves and seagrass, are not abundant at the subtidal part of BA (Wolff and Smit, 1990; Hemminga and Nieuwenhuize, 1991; Wolff et al., 1993b). In addition, MPB were assumed to only be an important primary producer in the seagrass-covered intertidal flat area of BA (Honkoop et al., 2008).

3. Results

3.1. Sea surface temperature and Chl a data

SST and surface Chl *a* concentrations were estimated by analyzing satellite images of the whole BA acquired during 2008. SST slightly decreased from April to May when the upwelling reached its maximum intensity, and then sharply increased in early summer when the intensity of the upwelling decreased (Fig. 2). This temporal trend seemed to be related to the distance from the upwelling area. Before June, sites 1 and 3 near Cape Blanc experienced lower seawater temperatures (i.e., stronger upwelling influence) than sites 6 and 9 close to the tidal flat area in the southeast (see Fig. 1). These spatial temperature differences were maximal (>2°C) during the intense upwelling periods from March to May. Figure 3 shows the spatial variability of SST and Chl *a* concentration (taken as a proxy for primary production) over BA at six dates from April 2008 to August 2008, corresponding to days with most readable Chl *a* data. The SST pattern clearly delimits the area around Cape Blanc where cold and nutrient-enriched water upwelled during strong NE wind periods. From March to May

2008, the cold water did not enter the southeastern part of BA and the spatial pattern in Chl *a* concentration indicated areas of major primary production that closely matched cold water areas (Figs. 2, 3). Overall, SST revealed that strong upwelling events occurred from March to May around Cape Blanc, which were quickly followed by high Chl *a* concentrations up to 25 mg m^3 (Fig. 3, top panel, May 3).

3.2. Isotopic signal of food sources and benthic invertebrates

Seagrass leaves, seagrass epiphytes, and MPB (pooled samples from seagrass-covered and bare patches) were clearly more ^{13}C-enriched than suspended POM and macroalgae (Table 2). POM exhibited large δ^{13}C variability among sampling sites, being most ^{13}C-enriched in the southern BA (Teichott) and within the tidal flat area (site 10). In the northern part of BA, POM was more ^{13}C-enriched in the western offshore side (sites 1, 2, and 3) than in the inshore eastern side (sites 5 and 7).

Eighty-eight taxa of benthic invertebrates with different trophic modes (mostly suspension feeders) were characterized for δ^{13}C and δ^{15}N along the offshore–inshore gradient (see Supplement 3). The mean δ^{13}C values per species per site for all suspension-feeding benthic invertebrates varied over a large range (~ 6‰) from Cape Blanc to the tidal flat (Fig. 4A). The δ^{15}N values varied in the same range (~ 6‰) over the same spatial area. Between-site differences were significant for both δ^{13}C and δ^{15}N (one-way ANOVA; $p < 0.001$ in both cases). However, δ^{13}C values discriminated between sampling sites much better than δ^{15}N values and allowed the identification of three distinct groups over the investigated area. Benthic suspension feeders living in the western offshore side of BA (sites 1 to 4) were clearly more ^{13}C-enriched than those living in the eastern inshore side (sites 5 to 8; Fig. 4A). This spatial pattern of δ^{13}C was even more pronounced when only selecting δ^{13}C data for species belonging to one of the three dominant families of suspension-feeders collected at

several sampling sites (mytilid bivalves, Fig. 4B; calyptreid gastropods, Fig. 4B; and venerid bivalves, Fig. 4C).

Mixing model computation applied to suspension-feeding invertebrates collected from sites 1 to 8 exhibited a much greater contribution of upwelling POM in the western offshore side of BA (sites 1 to 4) than in the eastern inshore side (sites 5 to 8; Fig. 5). The 0.95 confidence interval for upwelling POM ranged from 50 to 100% for sites 1 to 4 (mode ranging from 75 to 98%), while it ranged from 0 to 66% for sites 5 to 8 (mode ranging from 4 to 45%).

The spatial patterns of δ^{13}C of benthic invertebrates that belong to higher trophic levels (scavengers, omnivores, and predators), was similar to, though less marked than, those obtained for primary consumers (see Supplement 4), with higher δ^{13}C values in the northwestern (offshore) part compared to the southeastern (inshore) part of BA (Kruskal–Wallis test, $p < 0.01$; pairwise comparison Dunn's Method, $p < 0.05$). Secondary consumers collected near to the tidal flat (sites 9 and 10) exhibited more contrasting δ^{13}C values (from -19 to -10‰) than in the other two regions (equal variance test failed; $p < 0.05$). The δ^{15}N values of secondary consumers were significantly lower close to the tidal flat than in offshore and inshore areas (one-way ANOVA, $p < 0.001$; pairwise comparison Holm-Sidak method, $p < 0.05$ and $p = 0.50$, respectively).

3.3. Isotopic signal of fish

Forty-three species of fish with different trophic modes (mostly omnivorous or carnivorous) were characterized for δ^{13}C and δ^{15}N (see Supplement 5). Fish collected in the southern part of BA (Teichott) showed much higher δ^{13}C and lower δ^{15}N values than those collected in the northern subtidal part of the gulf (Nouadhibou and Arkeiss) (Figs. 6A and 6B). Considering all data (mean value per species per site), we found significant between-site δ^{13}C and δ^{15}N differences (one-way ANOVA, $p < 0.001$ in both cases). Fish from Teichott

were significantly more ^{13}C-enriched than fish from Nouadhibou and Arkeiss (Holm–Sidak pairwise multiple comparison, $p < 0.05$ in both cases), whereas δ^{13}C values for the latter two sites were almost significantly different ($p = 0.050$). Similarly, δ^{15}N values for fish from Teichott were significantly lower than those from Nouadhibou and Arkeiss (Holm–Sidak pairwise multiple comparison, $p < 0.05$ in both cases), but δ^{15}N values for fish from the latter two sites were almost significantly different ($p = 0.050$). The results of these statistical tests remained unchanged when considering only carnivorous fish species at all sites.

This isotopic discrepancy between north and south BA was even more evident when considering the eight taxa of fishes collected at Teichott and at least one of the two northern sites (Nouadhibou, Arkeiss) (Fig. 6A). The δ^{13}C and δ^{15}N values for flatfish *Psettodes* spp. had significant between-site differences (Kruskal–Wallis test, $p < 0.01$ in both cases), and pairwise multiple comparisons showed that individuals from Teichott were significantly more ^{13}C-enriched and ^{15}N-depleted than those from Nouadhibou and Arkeiss ($p < 0.05$ in all cases). Spatial differences in δ^{13}C and δ^{15}N values remained consistent for the omnivorous *Diplodus* spp. as well as the top predators *Pseudotolithus* spp. and *Pomadasys* spp. (Fig. 6A). Conversely, *U. canariensis* specimens from Teichott were significantly more ^{13}C-depleted than specimens from Nouadhibou (t-test, $p < 0.001$).

4. Discussion

We used complementary lines of evidence to assess the spatial extent of the trophic influence of the upwelling in the BA. First, satellite Chl *a* data suggested that in 2008 upwelling production was most available to benthic consumers from March to the end of May and in the northwestern edge of BA, where several pronounced plumes of high Chl *a* concentrations were observed. However, remote sensing Chl *a* data were available for only a few days per month during the investigated period because perfect atmospheric conditions are required. Second, SST data were obtained daily and allowed indirect identification of

14

upwelling areas with high phytoplankton biomass via visualization of coldest water zones. Third, we used $\delta^{13}C$ and $\delta^{15}N$ signals as trophic tracers to assess the main food sources that consumers of BA assimilated during the maximum intensity period of the Mauritanian upwelling.

Our stable isotope approach has been validated for many coastal ecosystems where co-existing potential food sources are distinguishable by their $\delta^{13}C$ values (Fry, 2006), and consumers are only weakly ^{13}C-enriched (< 1‰) with respect to their diet (Vander Zanden and Rasmussen, 2001; Post, 2002; Yokoyama et al., 2005). In BA, pelagic primary production was clearly more ^{13}C-depleted (< -18‰) than benthic microalgae, seagrass epiphytes, and seagrasses (> -14‰). Furthermore, the $\delta^{13}C$ signal allowed us to distinguish phytoplankton originating from the upwelling region (-18 to -16‰) from open ocean phytoplankton (-22 to -18‰) as observed in other upwelling systems (Fry and Wainright, 1991; Pancost et al., 1997; Allan et al., 2010). Such $\delta^{13}C$ variation can be explained by factors linked to the relative productivity of the system. In intense upwelling regions, a high phytoplankton growth rate and diatom predominance result in less fractionation against ^{13}C isotopes, and subsequently higher $\delta^{13}C$ values, than usually observed in open oceans (Rau et al., 2001). Accordingly, high $\delta^{13}C$ values obtained for POM in the northwest BA corresponded to areas where the highest Chl a concentration (10–25 mg m^{-3}) was observed during May 2008. Although we analyzed POM $\delta^{13}C$ only at the end of May, the ^{13}C-enriched trace of primary production in the upwelling should have persisted throughout the spring (Bode et al., 2003; Woodworth et al., 2004), allowing us to detect its incorporation into the BA subtidal benthic food web. We assessed the spatial influence of primary production that originates from the upwelling using sessile (or sedentary) subtidal suspension-feeding consumers which are good integrators of locally available food conditions and whose isotopic ratios provide a large-scale view of the main assimilated food source (Barnes and Jennings, 2009). The signals of suspension-

feeding bivalves, which represented most of our samples in the subtidal BA, is likely

integrated over at least 3 months according to recent controlled feeding experiments (Paulet et

al., 2006; Dubois et al., 2007) and field studies (Raikow and Hamilton, 2001; Carlier et al.,

2007).

When considering the subtidal area of BA north of the tidal flats (i.e., sites 1 to 8), the

$\delta^{13}C$ pattern of benthic primary consumers showed two distinct geographic zones. In the

northwest ^{13}C-enriched zone (sites 1 to 4), suspension-feeders clearly benefited from offshore

upwelling-driven phytoplankton production; the minimum contribution of upwelling-POM to

their diet ranged from 50% at site 2 to 80% at site 1. On the inshore side of BA (i.e., sites 5 to

8), benthic primary consumers exhibited low $\delta^{13}C$ values, suggesting that they depend on

autochthonous POM, with a classic oceanic $\delta^{13}C$ signal (< -20‰), and do not benefit from the

primary production of the upwelling. Accordingly, the ^{13}C-enrichment obtained at sites 1 to 4

closely matched the area where the coldest water and highest Chl *a* concentrations were

observed in spring 2008, whereas remote sensing Chl *a* data indicated that the southeastern

BA exhibited much less phytoplankton biomass. Overall, our $\delta^{13}C$ data suggest that, during

spring, the suspension-feeding benthic community living in the northwest subtidal area was

fueled mainly by upwelling-driven primary production, and that in the southeast subtidal area

of BA it was fueled mainly by autochthonous POM.

Our results corroborate previous direct Chl *a* measurements over the entire gulf and

the observation that upwelling-characteristic diatom species are lacking in the eastern BA

(Sevrin-Reyssac, 1993). Following the only available hydrodynamic model for BA (Peters,

1976), the inshore ^{13}C-depleted pattern may have resulted from changes in the species

composition of the phytoplankton community as upwelled waters moved from NW to NE and

then south. Similarly, a shift from a diatom-dominated to a dinoflagellate-dominated

phytoplankton community could explain an isotopic shift in mussel tissue downstream of an

upwelling cell in southern Africa (Allan et al., 2010). When considering the overall δ^{13}C

pattern of conspicuous species of suspension feeders and the outputs of the mixing model, the

trophic influence of the upwelling seemed to reach its southeastern limit between sites 4 and

6, west of the very shallow (< 5 m) north–south-oriented sand banks. According to Peters

(1976), a well defined and quasi-stationary water front existing along the southwestern edge

of BA would prevent any advection of upwelling-driven phytoplankton bloom into the inner

BA. The δ^{13}C shift between the 'offshore' upwelling area (sites 1 to 4) and the eastern coastal

side (sites 5 to 8) was still consistent for deposit feeders despite a low number of samples (see

Supplement 3). A similar spatial difference in δ^{13}C was also detected for benthic invertebrates

belonging to higher trophic levels (omnivores, scavengers, and predators), but the relative

trophic influence of the upwelling on these feeding guilds is less clear because of more

opportunistic feeding strategies, resulting in a blurring effect of the cumulative ^{13}C-

enrichment of consumer diets at the top of the benthic food web.

Benthic primary consumers collected at the northern entrance of the large seagrass-

covered intertidal flat area (sites 9 and 10) had heterogeneous δ^{13}C values (from -20 to -14‰)

that were more difficult to interpret than those obtained in the rest of BA. Given the rapid

decrease in the incorporation of upwelling-fuelled POM in benthic suspension feeders from

northwest to southeast BA, and that hydrodynamic knowledge indicates that water moves

mainly from site 4 to site 9 (Peters, 1976), it seems unlikely that upwelling-driven POM

contributed to the benthic community at sites 9 and 10, which were both located in the

intertidal part of BA. Living in the sediment-water interface where physical forces (i.e., wind

and tidal action) can be high, benthic diatoms often become suspended in the water column,

making them available to suspension-feeding organisms (de Jonge and van Beusekom, 1995).

Strong and alternate tidal currents around Iwik may have promoted the contribution of

resuspended MPB to the POM-assemblage in this intertidal part of BA. The δ^{13}C values for

benthic suspension feeders collected there can be explained by these animals consuming a mixed diet of δ^{13}C-depleted POM from the eastern inshore side (e.g., close to site 8) and δ^{13}C-enriched resuspended MPB from the intertidal flat. Notably, resuspended seagrass epiphytes could also contribute to the suspended POM pool in the intertidal part of BA, but given their low biomass, their contribution is expected to generally be low compared to resuspended MPB (Wolff et al., 1993b).

The highly variable δ^{13}C values obtained for benthic consumers collected at sites 9 and 10 (see Supplement 4) and for the suspension-feeding bivalve *Senilia senilis* at the intertidal flats surrounding the Iwik peninsula, which ranged from -19.9 to -12.5‰ (van der Geest, unpublished data from individuals collected in May 2008), agree with this hypothesis. In particular, the high δ^{13}C values at all trophic levels suggest a major trophic role of ^{13}C-enriched food sources in this tidal area (e.g., MPB, seagrass epiphyte, and/or recycled seagrass material). Thus, despite its close proximity, the southeastern area of BA remains outside the trophic influence of one of the most intense coastal upwelling zones worldwide. This situation contrasts with that of the northwestern coast of Galicia (northern part of the same Canary upwelling system), where benthic consumers inhabiting the coastline are mostly fuelled by the phytoplankton originating from the upwelling (Figueiras et al., 2002; Bode et al., 2006). Because the present study was performed in the spring following the maximum intensity upwelling event for the year, the marine part of PNBA is likely to be isolated from the upwelling inputs during the rest of the year.

It is important to question what the motile primary and secondary consumers with low isotopic turnover rates tell us about the long-term influence of upwelling-driven phytoplankton production on inshore BA food web functioning. Stable isotope ratios can be used to describe population mixing and migration patterns if animals move between areas with carbon source pools that have naturally distinct isotopic signatures (Fry, 1983). Here,

δ^{13}C ranges of offshore upwelling-driven primary production and inshore benthic primary production were clearly distinguishable. Based on the isotopic turnover rates acquired for adult fish in controlled laboratory experiments (Hesslein et al., 1993; MacAvoy et al., 2001), we assumed that motile consumer specimens collected during the present study had integrated the isotopic signal of their diet over at least 6 months (probably more than a year). Thus, isotopic signatures of fish dorsal muscles (with a slow turnover rate) gave us a longer time–integrated view of what fuels the BA food web than the isotopic signatures of invertebrate tissues. They indicated whether the fish had isotopically distinct regions where they had foraged during their life, and whether they were caught in their main feeding area (Suring and Wing, 2009).

The small pelagic planktivorous clupeids (*Sardinella* spp.; *Ethmalosa fimbriata*) are mostly encountered along the western edge of BA (south of Cape Blanc), where they feed on upwelling-driven primary production (Boély and Fréon, 1989; Cury et al., 2000, Arístegui et al., 2009). Here, these species exhibited consistent isotopic signals with a diet based mostly on upwelling-originated POM (see Supplement 4). Their δ^{13}C values closely matched those of the benthic suspension feeders collected northwest of BA, and their δ^{15}N values were in the upper range of those for benthic suspension feeders (or greater for *E. fimbriata*), probably because of a larger contribution of δ^{15}N-enriched zooplankton to their diet. Thus, isotopic data for planktivorous clupeids was a reliable reference for assessing whether other fish species belong to the same upwelling trophic pathway. Most of the species collected at Nouadhibou and Arkeiss probably depend on offshore pelagic (i.e., upwelling) production. The bimodal δ^{13}C pattern obtained for Arkeiss could indicate two distinct pathways, reflecting the slight δ^{13}C difference between upwelling and classical offshore primary production. However, although this pattern was evident at the POM and suspension feeder levels, extrapolation to top predators would need a more replicated and spatially controlled sampling strategy.

19

Most of the fishes collected around Teichott were more ^{13}C-enriched and ^{15}N-depleted than fishes collected in the northern part of BA, even when considering carnivorous species. The clear gradient in north–south δ^{13}C for each feeding guild strongly suggests that ^{13}C-enriched primary producers (MPB and, to a lesser extent, seagrass epiphytes) play a major trophic role in the tidal flat food web (i.e., fishes and their prey), but do not fuel the food web in the northern subtidal part of BA. Very large δ^{15}N differences obtained for some taxa (e.g., the top predator flatfish *Psettodes* spp.) suggest that these fish also feed at lower trophic levels around Teichott. Isotopic signals recorded for motile top predators, and some benthic invertebrates, indicate that benthic primary production represents the paramount food source for consumers inhabiting the tidal flat ecosystem. Therefore, the productivity of local benthic primary producers is likely large enough to support the related fish and shorebirds biomass in southeastern BA (Clavier et al., 2014) without any allochthonous organic matter inputs (e.g., upwelling-driven primary production). Our results reinforce the conclusions of recent studies of the functioning of this intertidal flat food web (Wolff et al., 1993a, 1993b, 2005). The large north–south differences in δ^{15}N obtained for fishes belonging to different feeding guilds, as well as carnivorous benthic invertebrates, can be explained by more ^{15}N-depleted food sources in southeastern BA. Although few isotopic data were obtained for primary producers, a similar spatial δ^{15}N pattern was obtained for this first trophic level (Table 2). This could be explained on the basis of the BA food web being fuelled by distinct sources of dissolved inorganic nitrogen (DIN), such as the upwelling and inputs of Sahara dust in the gulf (Wolff et al., 1993b). If these likely important DIN sources can be discriminated by their δ^{15}N signal, it would be interesting to assess their relative contribution to primary production over the entire BA. This is an important ecological issue that deserves further investigation.

The isotopic records of fish gave us the first clues about the degree of trophic connectivity between the northern subtidal part and southern intertidal part of BA. The

relatively high δ^{13}C values for both omnivorous and carnivorous fish from Teichott indicate that most fish caught in this area depend on local benthic production. Nevertheless, some specimens (e.g., *U. canariensis*) may have foraged outside of the tidal flat system over the months preceding their catch. According to our data, connectivity is weak between the northern and southern fish assemblages of BA. Despite Arkeiss and Teichott being relatively close to each other, isotopic results suggest that the exchange of carnivorous and omnivorous fishes is limited, at least during the few months that preceded our sampling. However, the question of trophic connectivity between these fishing areas needs to be investigated further.

Given that we analyzed adult-sized specimens of fish whose diet signals had been integrated over several months, the clear north–south isotopic shift suggests that there are two main trophic pathways for top predators in BA. One is based on upwelling-driven primary production, which prevails in the northwestern part of the gulf. The other, based on autochthonous benthic primary production, is predominant in the intertidal flat area. This means that any natural or anthropogenic perturbation of this vast seagrass ecosystem could have major ecological consequences on its ecological functioning, and that no beneficial trophic influence of the upwelling can be expected. As offshore oil extraction projects are currently planned a few tens of km from the PNBA, our conclusions will be of value for the ongoing management of this unique and fragile marine ecosystem.

References

Ahmedou Salem, M.V., van der Geest, M., Piersma, T., Saoud, Y., van Gils, J.A., 2014. Seasonal changes in mollusc abundance in a tropical intertidal ecosystem, Banc d'Arguin (Mauritania): testing the 'shorebird depletion' hypothesis. Estuar. Coast. Shelf. Sci. 136, 26-34.

Allan, E.L., Ambrose, S.T., Richoux, N.B., Froneman, P.W., 2010. Determining spatial changes in the diet of nearshore suspension-feeders along the South African coastline: Stable isotope and fatty acid signatures. Estuar. Coast. Shelf. Sci. 87, 463–471.

Altenburg, W., Engelmoer, M., Mes, R., Piersma, T., 1982. Wintering waders on the Banc d'Arguin, Mauritania. Report of the Netherlands Ornithological Expedition 1980. Stichting Veth tot Steun aan Waddenonderzoek, Leiden.

Arístegui, J., Alvarez-Salgado, X., Barton, E., Figueiras, F., Hernández-León, S., Roy, C., Santos, A., 2006. Oceanography and fisheries of the Canary Current/Iberian region of the eastern North Atlantic. In: Robinson, A.R., Brink, K.H., eds. The Global Coastal Ocean. Interdisciplinary Regional Studies and Synthesis. Cambridge: Harvard University Press. pp.877–931.

Arístegui, J., Barton, E.D., Álvarez-Salgado, X.A., Santos, A.M.P., Figueiras, F.G., Kifani, S., Hernández-León, S., Mason, E., Machú, E., Demarcq, H., 2009. Sub-regional ecosystem variability in the Canary Current upwelling. Progr. Oceanogr. 83,33–48.

Barnes, C., Jennings, J.T.B., 2009. Environmental correlates of large-scale spatial variation in the $\delta^{13}C$ of marine animals. Estuar. Coast. Shelf Sci. 81, 368–374.

Bode, A., Carrera, P., Lens, S., 2003. The pelagic foodweb in the upwelling ecosystem of Galicia (NW Spain) during spring: natural abundance of stable carbon and nitrogen isotopes. ICES J. Mar. Sci. 60, 11–22.

Bode, A., Alvarez-Ossorio, M.T., Varela, M., 2006. Phytoplankton and macrophyte contributions to littoral food webs in the Galician upwelling estimated from stable isotopes. Mar. Ecol. Prog. Ser. 318, 89–102.

Boély, T., Fréon, P., 1980. Coastal pelagic resources. In: Troadec, J.P., Garcia, S., editors. The fish resources of the eastern central Atlantic. Part one: The resources of the Gulf of Guinea from Angola to Mauritania. Rome: FAO. pp.13-76.

Bosley, K.L., Witting, D.A., Chambers, R.C., Wainright, S.C., 2002. Estimating turnover rates of carbon and nitrogen in recently metamorphosed winter flounder *Pseudopleuronectes americanus* with stable isotopes. Mar. Ecol. Prog. Ser. 236, 233–240.

Carlier, A., Riera, P., Amouroux, J.M., Bodiou, J.-Y., Escoubeyrou, K., Desmalades, M., Caparros, J., Grémare, A., 2007. A seasonal survey of the food web in the Lapalme Lagoon (northwestern Mediterranean) assessed by carbon and nitrogen stable isotope analysis. Estuar. Coast. Shelf Sci. 73, 299–315.

Christensen, J.P., Packard, T.T., 1977. Sediment metabolism from the northwest African upwelling system. Deep Sea Research 24, 331–343.

Clavier, J., Chauvaud, L., Amice, E., Lazure, P., van der Geest, M., Labrosse, P., Diagne, A., Carlier, A., Chauvaud, S., 2014. Benthic metabolism in shallow coastal ecosystems of the Banc d'Arguin, Mauritania. Mar. Ecol. Prog. Ser. 501, 11-23.

Cloern, J.E., 1982. Does the benthos control phytoplankton biomass in south San Francisco Bay? Mar. Ecol. Prog. Ser. 9, 191–202.

Couch, C.A., 1989. Carbon and nitrogen stable isotopes of meiobenthos and their food resources. Estuar. Coast. Shelf Sci. 28, 433–441.

Cury, P., Bakun, A., Crawford, R.J.M., Jarre, A., Quiñones, R.A., Shannon, L.J., Verheye, H.M., 2000. Small pelagics in upwelling systems: patterns of interaction and structural changes in "wasp-waist" ecosystems. ICES J. Mar. Sc. 57, 603–618.

Dedah, S., 1993. Wind, surface water temperature, surface salinity and pollution in the area of the Banc d'Arguin, Mauritania. Hydrobiologia 258, 9–19.

de Jonge, V.N., van Beusekom, J.E.E., 1995. Wind- and tide-induced resuspension of sediment and microphytobenthos from tidal flats in the Ems estuary. Limnol. Oceanogr. 40, 766-778.

Dubois, S., Jean-Louis, B., Bertrand, B., Lefebvre, S., 2007. Isotope trophic-step fractionation of suspension-feeding species: Implications for food partitioning in coastal ecosystems. J. Exp. Mar. Biol. Ecol. 351, 121–128.

Duineveld, G.C.A., Lavaleye, M.S.S., Noort, G.J., 1993. The trawlfauna of the Mauritanian shelf (Northwest Africa): density, species composition, and biomass. Hydrobiologia 258, 165–173.

Engelmoer, M., Piersma, T., Altenburg, W., Mes, R., 1984. The Banc d'Arguin (Mauritania), in: Evans, P.R., Goss-Custard, J.D., Hale, W.G. (Eds.), Coastal waders and wildfowl in winter. Cambridge University Press, Cambridge, pp. 293-310.

Farikou, O., Sawadogo, S., Niang, A., Brajard, J., Mejia, C., Crépon, M., Thiria, S., 2013. Multivariate Analysis of the Senegalo-Mauritanian Area by Merging Satellite Remote Sensing Ocean Color and SST Observations. Research Journal of Environmental and Earth Sciences 5(12), 756-768.

Figueiras, F.G., Labarta, U., Fernández Reiriz, M.J., 2002. Coastal upwelling, primary production and mussel growth in the Rías Baixas of Galicia. Hydrobiologia 484, 121-131.

Fry, B., 1983. Fish and shrimp migrations in the northern Gulf of Mexico analyzed using stable C, N and S isotope ratios. Fish. Bull. 81, 789–801.

Fry, B., 2006. Stable Isotope Ecology. Springer Verlag. p 308.

Fry, B., Wainright S.C.W., 1991. Diatom sources of ^{13}C-rich carbon in marine food webs. Mar. Ecol. Prog. Ser. 76, 149–157.

Gohin, F., 2011. Annual cycles of chlorophyll-a, non-algal suspended particulate matter, and turbidity observed from space and in-situ in coastal waters. Ocean Sci. 7, 705–732.

Hesslein, R.H., Hallard, K.A., Ramlal, P., 1993. Replacement of sulfur, carbon, and nitrogen in tissue of growing broad whitefish (*Coregonus nasus*) in response to a change in diet traced by δ^{34}S, δ^{13}C and δ^{15}N. Can. Journ. Fish. Aquat. Sci. 50, 2071–2076.

Hemminga, M.A., Nieuwenhuize, J., 1991. Transport, deposition and *in situ* decay of seagrasses in a tropical mudflat area (Banc d'Arguin, Mauritania). Neth. J. Sea Res. 27, 183-190.

Honkoop, P.J.C., Berghuis, E.M., Holthuijsen, S., Lavaleye, M.S.S., Piersma, T., 2008. Molluscan assemblages of seagrass-covered and bare intertidal flats on the Banc d'Arguin, Mauritania, in relation to characteristics of sediment and organic matter. J. Sea Res. 60, 255–263.

Jackson, A.L., Inger, R., Parnell, A.C., Bearhop, S., 2011. Comparing isotopic niche widths among and within communities: SIBER–Stable Isotope Bayesian Ellipses in R. J. Anim. Ecol. 80, 595–602.

Jager, Z., 1993. The distribution and abundance of young fish in the Banc d'Arguin, Mauritania. Hydrobiologia 258, 185–196.

Josse, E., 1989. Les ressources halieutiques de la ZEE mauritanienne. Description, évaluation et aménagement. Rapport du deuxième groupe de travail CNROP/FAO/ORSTOM. Rome: FAO. p222.

Lathuiliere, C., Echevin, V., Levy, M., 2008. Seasonal and intraseasonal surface chlorophyll-a variability along the northwest African coast. J. Geophys. Res. 113, C05007.

Loktionov, Y., 1993. Hydrographical observations west of the Banc d'Arguin, Mauritania, in May 1988. Hydrobiologia 258, 21–32.

MacAvoy, S.E., Macko, S.A., Garman, G.C., 2001. Isotopic turnover in aquatic predators: quantifying the exploitation of migratory prey. Can. Journ. Fish. Aquat. Sci. 58, 923–932.

Minas, H., Codispoti, L., Dugdale, R., 1982. Nutrients and primary production in the upwelling region off Northwest Africa. Rapp. Pv. Reun. CIEM 180, 148-183.

Mittelstaedt, E., 1991. The ocean boundary along the northwest African coast: Circulation and oceanographic properties at the sea surface. Progr. Oceanogr. 26, 307–355.

Pancost, R.D., Freeman, K.H., Wakeham, S.G., Robertson, C.Y., 1997. Controls on carbon isotope fractionation by diatoms in the Peru upwelling region. Geoch. Cosmoch. Acta 61, 4983–4991.

Parnell, A.C., Inger, R., Bearhop, S., Jackson, A.L., 2010. Source partitioning using stable isotopes: coping with too much variation. PloS One 5, e9672.

Paulet, Y.M., Lorrain, A., Richard, J., Pouvreau, S., 2006. Experimental shift in diet δ^{13}C: A potential tool for ecophysiological studies in marine bivalves. Org. Geochem 37, 1359–1370.

Peters, H., 1976. The spreading of water masses of the Banc d'Arguin in the upwelling area of the Northern Mauritanian coast. "'Meteor'" Forschungsergebnisse (A) 18, 78–100.

Post, D.M., 2002. Using stable isotopes to estimate trophic position: models, methods, and assumptions. Ecology 83, 703–718.

Raikow, D.F., Hamilton, S.K., 2001. Bivalve diets in a midwestern U.S. stream: A stable isotope enrichment study. Limnol. Oceanogr. 46, 514–522.

Rau, G.H., Chavez, F.P., Friederich, G.E., 2001. Plankton $^{13}C/^{12}C$ variations in Monterey Bay, California: evidence of non-diffusive inorganic carbon uptake by phytoplankton in an upwelling environment. Deep Sea Res. I 48, 79–94.

Schaffmeister, B.E., Hiddink, J.G., Wolff, W.J., 2006. Habitat use of shrimps in the intertidal and shallow subtidal seagrass beds of the tropical Banc d'Arguin, Mauritania. J. Sea Res. 55, 230–243.

Sevrin-Reyssac, J., 1993. Hydrology and underwater climate of the Banc d'Arguin, Mauritania: a review. Hydrobiologia 258, 1–8.

Smit, C.J., Piersma, T., 1989. Numbers, mid-winter distribution and migration of wader populations using the East Atlantic Flyway. IWRB Special Publ. 9, 24–63.

Suring, E., Wing, S.R., 2009. Isotopic turnover rate and fractionation in multiple tissues of red rock lobster (*Jasus edwardsii*) and blue cod (*Parapercis colias*): Consequences for ecological studies. J. Exp. Mar. Biol. Ecol. 370, 56–63.

Sweeting, C.J., Barry, J., Barnes, C., Polunin, N.V.C., Jennings, S., 2007. Effects of body size and environment on diet-tissue $\delta^{15}N$ fractionation in fishes. J. Exp. Mar. Biol. Ecol. 340, 1-10.

Van Camp, L., Nykjaer, L., Mittelstaedt, E., Schlittenhardt, P., 1991. Upwelling and boundary circulation off Northwest Africa as depicted by infrared and visible satellite observations. Progr. Oceanogr. 26, 357–402.

van der Geest, M., 2013. Multi-trophic interactions within the seagrass beds of Banc d'Arguin, Mauritania: a chemosynthesis-based intertidal ecosystem, PhD Thesis, University of Groningen, Groningen, The Netherlands.

Vanderklift, M.A., Ponsard, S., 2003. Sources of variation in consumer-diet δ^{15}N enrichment: a meta-analysis. Oecologia 136, 169–182.

Vander Zanden, M.J., Rasmussen, J.B., 2001. Variation in δ^{15}N and δ^{13}C trophic fractionation: Implications for aquatic food web studies. Limnol. Oceanogr. 46, 2061–2066.

Wolff, W.J., Duiven, A.G., Duiven, P., Esselink, P., Gueye, A., Meijboom, A., Moerland, G., Zegers, J., 1993a. Biomass of macrobenthic tidal flat fauna of the Banc d'Arguin, Mauritania. Hydrobiologia 258, 151–163.

Wolff, W.J., Land, J., Nienhuis, P.H., Wilde, P.A.W.J., 1993b. The functioning of the ecosystem of the Banc d'Arguin, Mauritania: a review. Hydrobiologia 258, 211–222.

Wolff, W.J., Michaelis, H., 2008. Do shorebirds graze down zoobenthic biomass at the Banc d'Arguin tidal flats in Mauritania? Estuar. Coast. Shelf Sci. 79, 491–495.

Wolff, W.J., Smit, C.J., 1990. The Banc d'Arguin, Mauritania, as an environment for coastal birds. Ardea 78, 17–38.

Wolff, W.J., Van Etten, J.P.C., Hiddink, J.G., Montserrat, F., Schaffmeister, B.E., Vonk, J.A., De Vries, A.B., 2005. Predation on the benthic fauna of the tidal flats of the Banc d'Arguin (Mauritania). In: Symoens, J.J. Eds. Coastal Ecosystems of West-Africa Biological Diversity-Resources-Conservation. Brussels. pp.43–59.

Woodworth, M., Goñi, M., Tappa, E., Tedesco, K., Thunell, R., Astor, Y., Varela, R., Rafael Diaz-Ramos, J., Müller-Karger, F., 2004. Oceanographic controls on the carbon isotopic compositions of sinking particles from the Cariaco Basin. Deep Sea Res. I 51, 1955–1974.

Yokoyama, H., Tamaki, A., Harada, K., Shimoda, K., Koyama, K., Ishihi, Y., 2005. Variability of diet–tissue isotopic fractionation in estuarine macrobenthos. Mar. Ecol. Prog. Ser. 296, 115–128.

Yokoyama, H., Ishihi, Y., Yamamoto, S., 2008. Diet-tissue isotopic fractionation of the Pacific oyster *Crassostrea gigas*. Mar. Ecol. Prog. Ser. 358, 173–179.

TABLES

Table 1: Sample collection details

Sites		Sample types	Latitude	Longitude	Sampling dates	Depth (m)	Bottom characteristics
1	close to Cape Blanc	BI; POM	20°46'00" N	17°04'00" W	May 22, 2008	17	calcareous blocks; coarse sand
2	-	BI; POM	20°51'95" N	17°02'03" W	May 26, 2008	10	coarse sand; maerl
3	-	BI	20°28'28" N	16°57'78" W	May 23, 2008	10	shell sand; *Venus rosalina* shells; calcareous algae
4	-	BI	20°07'14" N	16°45'20" W	May 25, 2008	8	shell sand
5	-	BI; POM; SG	20°38'71" N	16°43'39" W	May 23, 2008	8	shell sand
6	-	BI	20°11'21" N	16°33'50" W	May 25, 2008	15	mud
7	-	BI; POM	20°12'84" N	16°14'12" W	May 25, 2008	8	muddy sand
8	-	BI; POM	20°02'63" N	16°20'96" W	May 24, 2008	9	muddy sand
9	front of Iwik village	BI	19°52'34" N	16°18'16" W	May 24, 2008	5	muddy sand (channel with strong tide current)
10	vicinity of Iwik village	BI; POM; SG	19°53'02" N	16°17'34" W	May 19, 2008	intertidal	fine sand; *Zostera noltii* bed
10	vicinity of Iwik village	EP	19°53'02" N	16°17'34" W	May 8-13, 2008	intertidal	*Zostera* and *Cymodocea* epiphytes
10	vicinity of Iwik village	MPB	19°53'02" N	16°17'34" W	May 8-14, 2008	intertidal	4 bare sand and 4 seagrass-covered muddy sites
10	vicinity of Iwik village	POM; SG; EP	19°53'02" N	16°17'34" W	February 1, 2010	intertidal	fine sand; *Zostera* and (subtidal) *Cymodocea* beds
N	Nouadhibou harbor	fishes; POM	-	-	May 22, 2008	-	-
A	Arkeiss village	fishes; POM	-	-	May 24, 2008	-	-
T	Teichott village	fishes; POM	-	-	May 25, 2008	-	-

BI: benthic invertebrates; POM; suspended particulate organic matter; SG: seagrass; EP: seagrass epiphytes; MPB: microphytobenthos.

30

Table 2: Mean δ^{13}C and δ^{15}N values ($\pm$ SD, when $n > 2$) of potential sources of organic matter collected at each sampling site.

OM sources	Site	n	δ^{13}C (‰)			δ^{15}N (‰)		
Macroalgae								
Rhodophyta	1, 4, 5	*3*	-19.4	$\pm$	1.8	8.2	$\pm$	0.4
Sargassum sp.	4	*1*	-17.6			8.1		
Seagrasses								
Zostera noltii	5	*1*	-9.9			8.3		
	10	*4*	-8.2	$\pm$	1.2	2.6	$\pm$	1.5
	10[a]	*18*	-8.4	$\pm$	0.5	2.8	$\pm$	1.0
Cymodocea nodosa	10	*1*	-6.9			1.3		
	10[a]	*6*	-7.6	$\pm$	0.4	3.9	$\pm$	0.3
Seagrass epiphytes	10	*8*	-11.2	$\pm$	3.6	2.2	$\pm$	1.6
	10[a]	*5*	-11.4	$\pm$	0.7	2.9	$\pm$	0.3
POM	1	*3*	-19.3	$\pm$	0.3	4.7	$\pm$	0.2
	2	*3*	-18.5	$\pm$	0.1	7.8	$\pm$	1.2
	3	*3*	-18.0	$\pm$	0.1	4.0	$\pm$	0.2
	5	*3*	-21.6	$\pm$	0.2	8.7	$\pm$	0.7
	7	*3*	-20.7	$\pm$	0.1	5.1[b]		
	10	*3*	-17.9	$\pm$	0.7	4.0	$\pm$	0.5
	10[a]	*21*	-18.4	$\pm$	1.0	1.2	$\pm$	0.7
	Teichott	*3*	-15.5	$\pm$	0.3	nd		
Microphytobenthos	10	*8*	-13.7	$\pm$	0.6	4.2	$\pm$	0.5

POM = suspended particulate organic matter; nd: no data available. Samples were collected in May 2008 unless otherwise noted.

[a] Samples were collected in February 2010.

[b] $n = 1$ for δ^{15}N because two analyses failed.

FIGURE CAPTIONS

Fig. 1: Map of the Banc d'Arguin showing the location of sampling sites for macrobenthos (black squares) and fishery landing sites where fish were recovered (open circles).

Fig. 2: Month-averaged sea surface temperatures (SST) in 2008 at sites 1, 3, 6, and 9 (see Fig. 1 for site locations). Data were averaged over a 100-km^2 area centered at each sampling site. The vertical grey bar indicates the period during which consumers (benthic invertebrates and fish) were collected for stable isotope analysis.

Fig. 3: Surface chlorophyll a concentration (mg m^{-3}; top panel) and sea surface temperature (°C; bottom panel) estimated from satellite images obtained on April 11, April 20, May 3, May 13, May 29, and August 26, 2008. Black areas correspond to a lack of data due to unsuitable atmospheric conditions. White circles in the bottom panel indicate the locations of sites 1, 3, 6, and 9. The dashed box indicates the period during which consumers (benthic invertebrates and fish) were collected for stable isotope analysis.

Fig. 4: A) Mean δ^{13}C values ($\pm$ SD) obtained for each suspension-feeding benthic invertebrate taxa and averaged per sampling site. The number of different taxa used per site is presented in brackets. See Appendix B for the list of benthic invertebrate taxa sampled. Dotted lines delimit three geographical areas with hypothesized distinct trophic regimes. B-D) Raw δ^{13}C values obtained for individuals from the most frequently encountered families of suspension feeders at Banc d'Arguin, from Cap Blanc in the northwest (site 1) to Iwik in the southeast (site 9). B (open triangles) = Mytilidae; C (open circles) = Calyptraeidae; D (open diamonds) = Veneridae.

Fig. 5: SIAR boxplots showing the proportional contribution (%) of POM from the upwelling area and POM from the inshore water to the diet of benthic suspension feeders (bivalves, sponges, polychaetes, brachiopods; $\delta^{13}C$ values were averaged across species) collected from sites 1 (close to the upwelling) to 8 (close to the entrance of the inshore tidal flat area). Each plot shows 95% (darkest grey), 75% (intermediate grey), and 25% (lightest grey) credibility intervals.

Fig. 6: A) Mean $\delta^{15}N$ and $\delta^{13}C$ values (± SD when n > 2) of eight taxa of fishes caught within at least two fishing areas (white symbols = Nouadhibou harbor; grey symbols = Arkeiss; black symbols = Teichott). The fish taxa classified into three trophic guilds were: 1 = *Sardinella* spp.; 2 = *Arius* spp.; 3 = *Diplodus sargus*; 4 = *Synaptura lusitanica*; 5 = *Psettodes* spp.; 6 = *Umbrina canariensis*; 7 = *Pseudotolithus* spp.; and 8 = *Pomadasys* spp. The standard ellipse area (SEA) calculated using SIBER (Jackson et al., 2011) represents the trophic niche width of all sampled carnivorous and omnivorous fish in each fishing area (dashed line: Nouadhibou, dot-dash line: Arkeiss, solid line: Teichott). Boxes represent the ranges of values obtained for potential food sources. Note that upwelling-POM isotope signatures reflect pooled values for sites 1 and 2, inshore-POM isotope signatures reflect pooled values for sites 5, 7, and 8, and tidal mudflat-POM isotope signatures reflect pooled values for site 10. Black dotted arrows and the grey area represent the range of the extent of ^{13}C and ^{15}N consumer-diet enrichment factors based on the mean values obtained for carnivorous marine organisms by Vander Zanden and Rasmussen (2001), Post (2002), Vanderklift and Ponsard (2003), and Sweeting et al. (2007). B) $\delta^{13}C$ frequency distribution for each fishing area when using the mean $\delta^{13}C$ values per fish species. Note that the three feeding guilds presented in Fig. 6A are included.
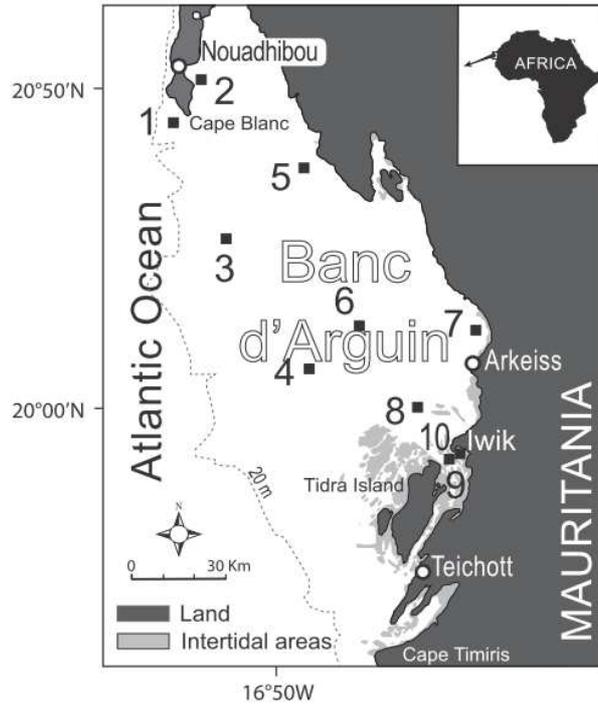
Fig. 1
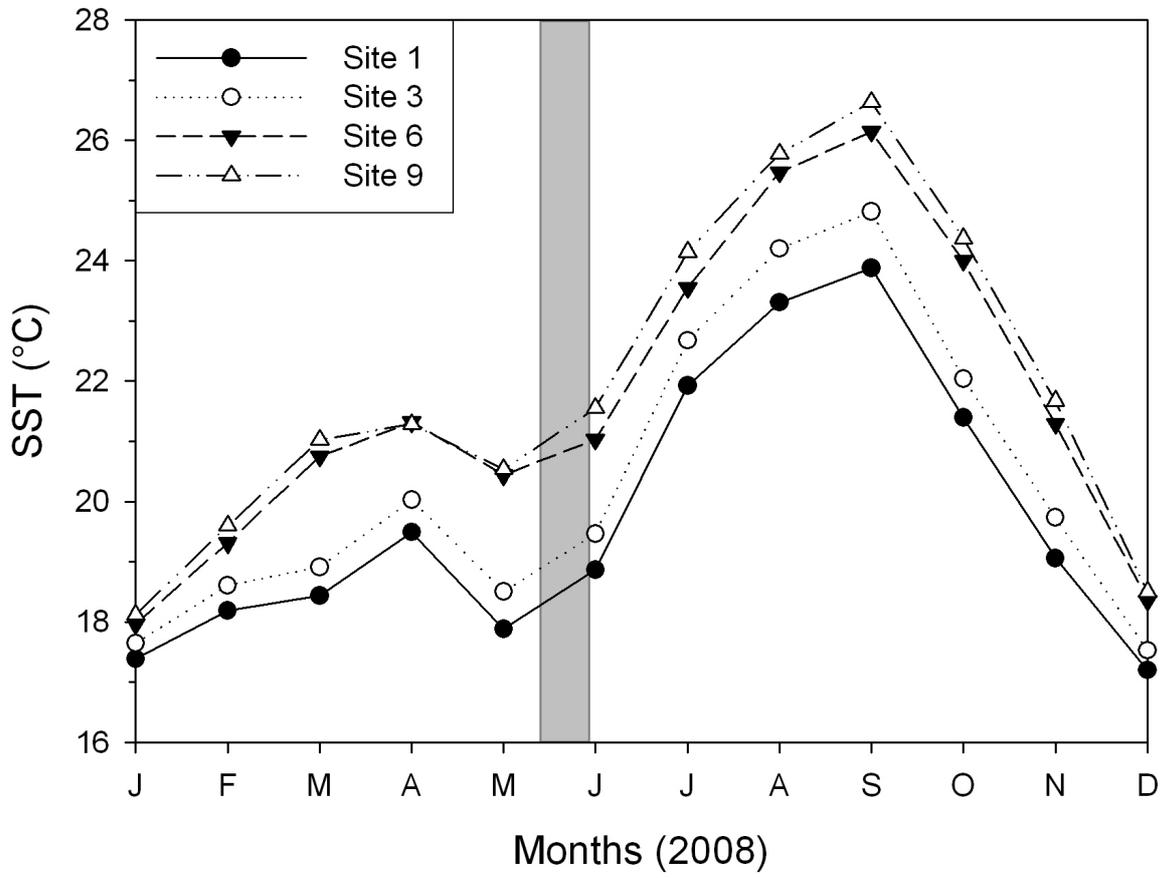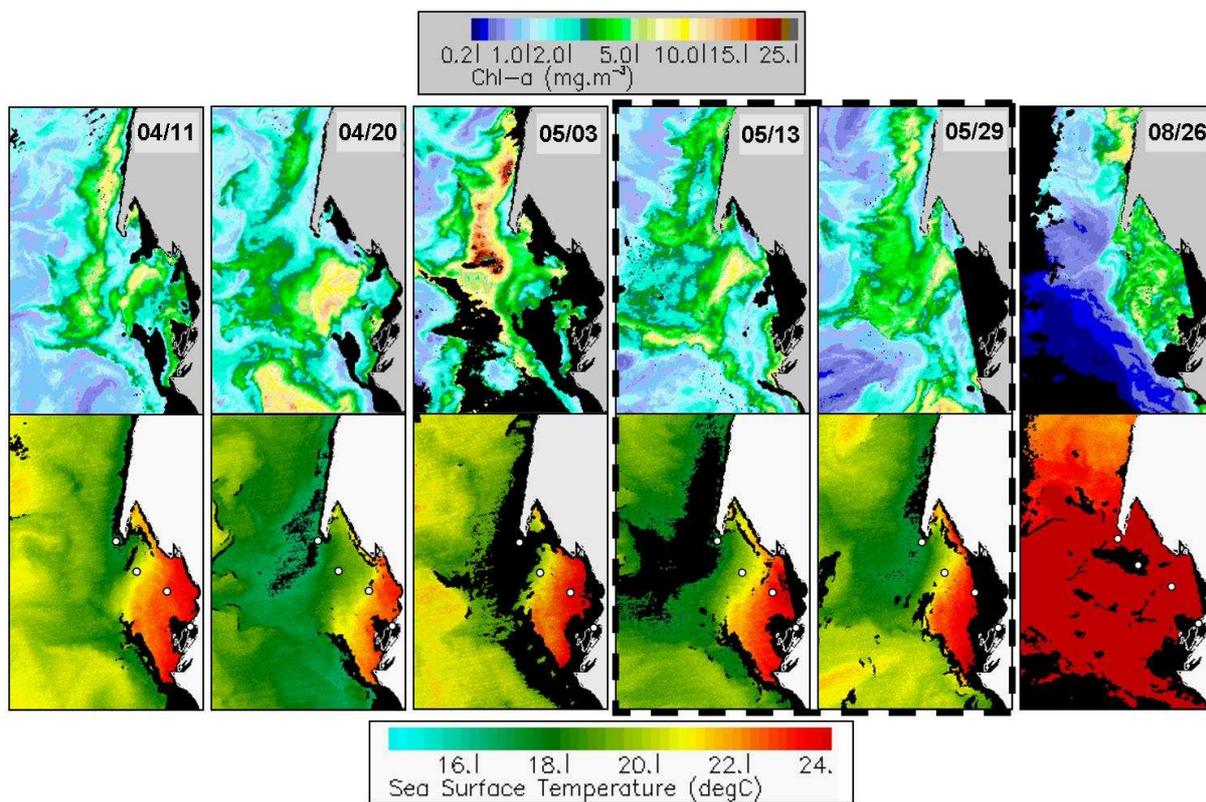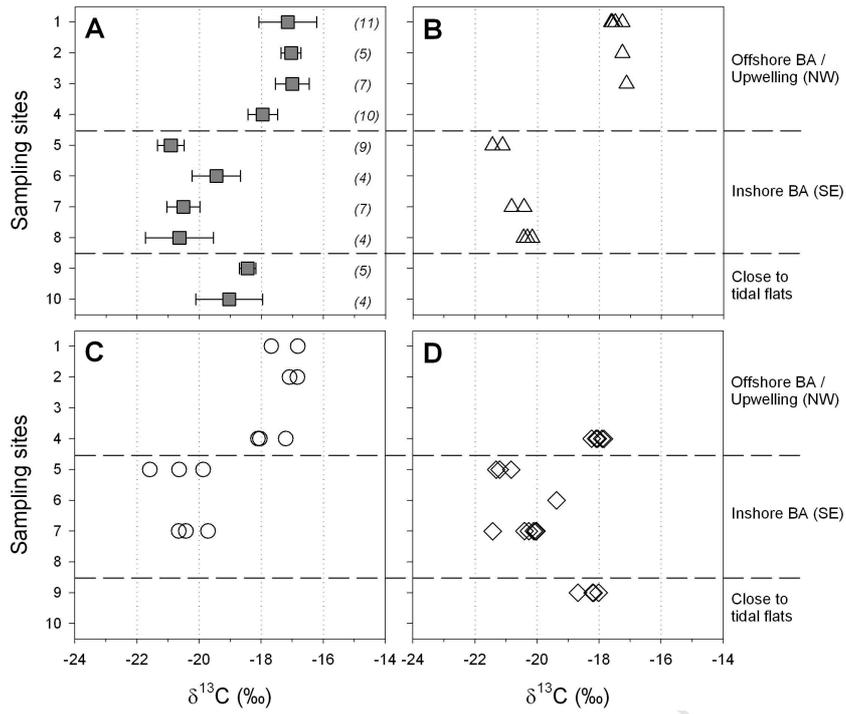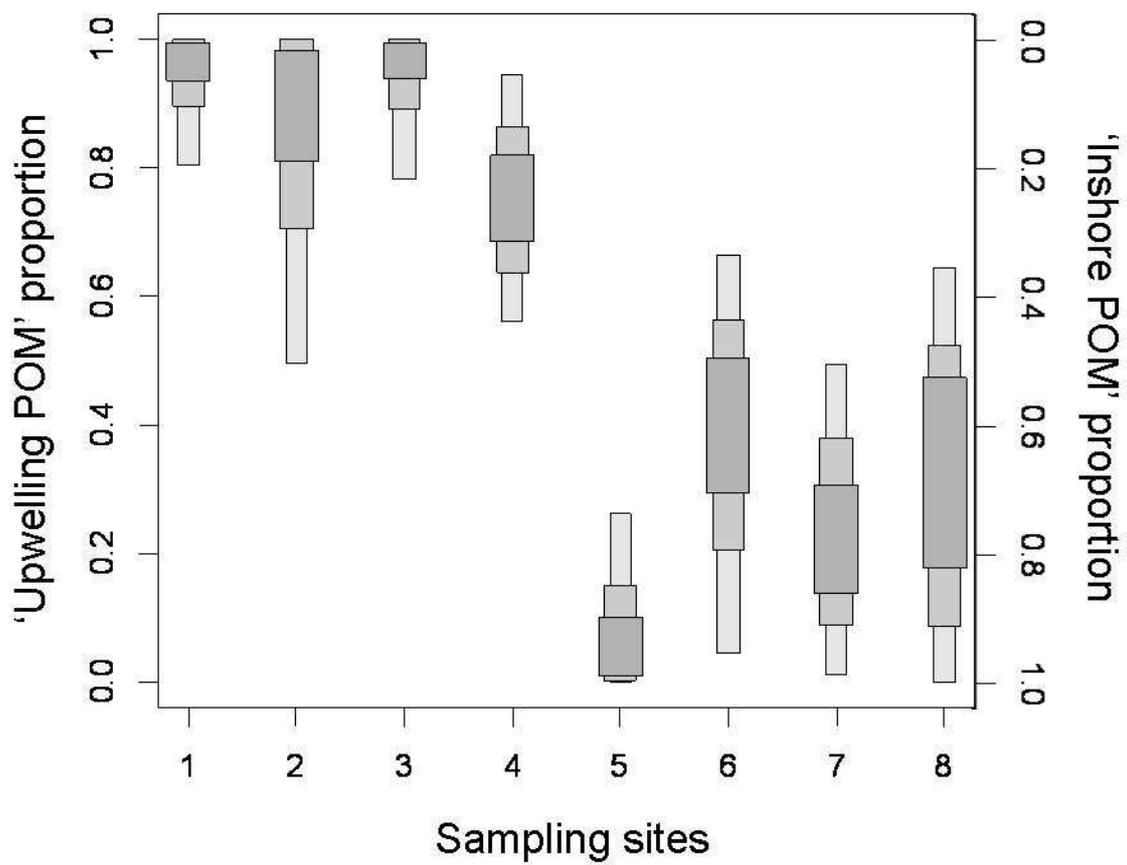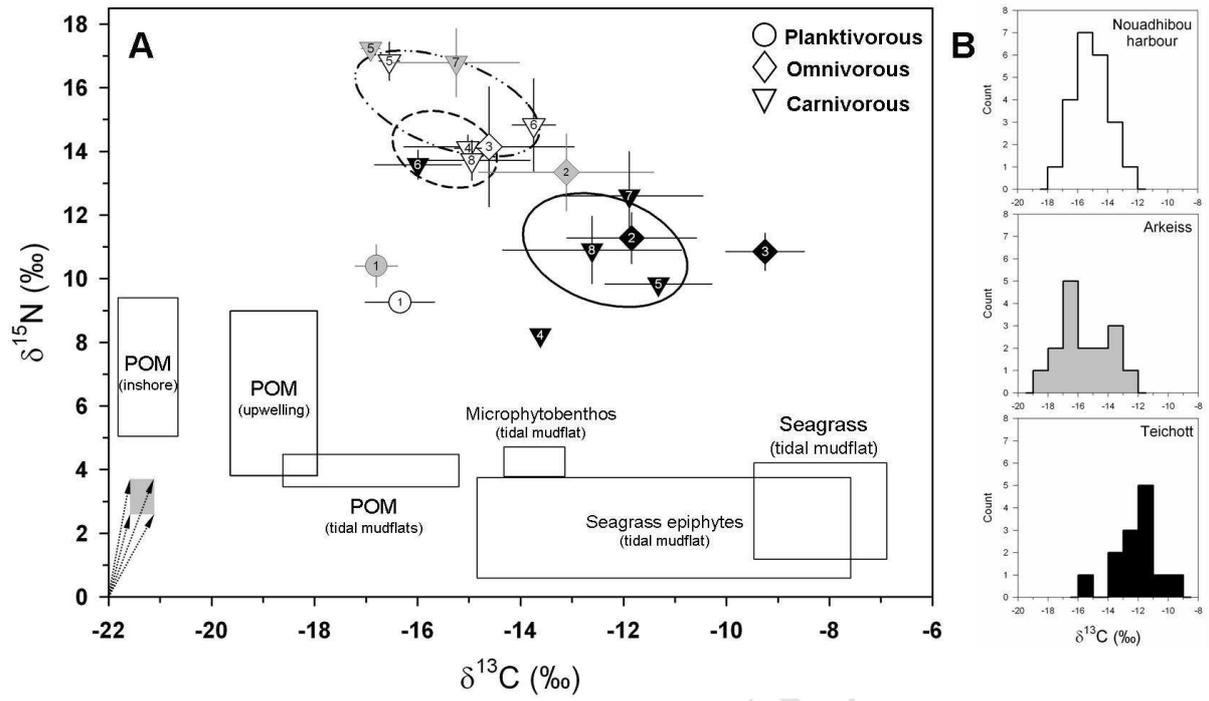
Highlights:

The Mauritanian upwelling only fuels the northwestern part of Banc d'Arguin food web.

Coupling remote sensing with stable isotope analysis to infer trophic connectivity.

Vast seagrass-covered intertidal flat supported by local benthic primary production.

Weak connectivity between the northern and southern fish assemblages of Banc d'Arguin.

Supplement 1: Methods used for sampling microphytobenthos (MPB)

Initially, a sample of the top 3-mm layer of sediment was collected where the brown–green color was most developed on the intertidal area. At the Iwik station, each sediment sample was covered with an 80-µm nylon mesh screen and GF/F-filtered seawater added until the mesh was covered. Combusted silica powder was placed on top of the mesh (1 cm) and GF/F-filtered seawater added again up to 1 cm above the silica powder surface. The samples were then covered with a transparent lid to prevent evaporation and contamination and placed in daylight to attract the diatoms through the filter into the silica powder. After 6 hours, the overlying water was removed and the silica powder with diatoms gently scraped off and put into a 250 ml Erlenmeyer flask. GF/F-filtered seawater was added to the flask, which was stirred manually until the diatoms were loosened from the silica particles. The supernatant containing diatoms was filtered into a precombusted GF/F filter, which was stored at -20°C before isotopic analysis.

Supplement 2: Stable isotope analysis

Stable isotope analyses of carbon and nitrogen were carried out using the elemental analysis–isotope ratio mass spectrometry method. Samples were analyzed by combustion in a Carlo Erba NC2500 Elemental Analyzer and delivered to a Finnigan Mat Delta Plus mass spectrometer (Thermo Finnigan, Bremen, Germany) via continuous flow. The precision for $\delta^{13}C$ and $\delta^{15}N$ was ~0.1‰ and ~0.4‰ (for samples with N content >5% dry weight), respectively. Data are reported as delta values relative to international standards Peedee Belemnite carbonate and atmospheric nitrogen and calibrated using International Atomic Energy Agency standards CH6 (-10.4‰), CH7 (-31.8‰), N1 (0.4‰), and N2 (20.5‰). Commercially available standards (acetanilide, nicotinamide, BLS, SMB-M, and peach leaf) were analyzed alongside the samples as quality-control. The standard deviation of the standards' isotopic values (used as a reproducibility expression) were <0.08‰ and <0.19‰ for $\delta^{13}C$ and $\delta^{15}N$, respectively. The C:N atomic ratios were calculated from the percentages of organic carbon and nitrogen obtained for decarbonated samples.

Supplement 3: Table

δ^{13}C of taxa of benthic invertebrates sampled during the present study (Mean values per taxa per site; for each taxa, the number of individuals

analyzed at each sampling site is indicated in italics). Trophic modes are suspension feeders (SF), interface feeders (IF), deposit feeders (DF),

subsurface deposit feeders (SSDF), grazers (Gr), and omnivorous/scavengers/predators (P). *Solemya togata* harbors endosymbiotic sulfur-

oxidizing bacteria (SOB).

Taxa	Trophic mode	Mean δ^{13}C per site *(number of replicate)*									
		1	2	3	4	5	6	7	8	9	10
Porifera											
Porifera sp. 1	SF	-16.2 *(3)*									
Porifera sp. 2	SF	-16.1 *(3)*									
Porifera sp. 3	SF	-15.9 *(2)*									
Porifera sp. 4	SF	-17.5 *(2)*									
Porifera sp. 5	SF	-17.8 *(5)*									
Porifera sp. 6	SF				-17.4 *(1)*						
Porifera sp. 7	SF			-17.1 *(1)*							
Bryozoa											
Bryozoa ind.	SF	-18.6 *(2)*									
Cnidaria											
Anemonia sulcata	P		-16.0 *(1)*								
Brachiopoda											
Lingula sp.	SF							-20.8 *(3)*			
Bivalvia											
Senilia senilis	SF										-19.8 *(7)*
Astarte fusca	SF		-16.8 *(1)*		-18.8 *(2)*						
Cardium ringens	SF					-20.4 *(3)*			-20.5 *(2)*	-18.2 *(1)*	
Laevicardium sp.	SF					-21.6 *(1)*					-17.8 *(2)*
Cardiocardita ajar	SF				-18.3 *(1)*		-20.4 *(1)*	-21.2 *(1)*			
Chama crenulata	SF	-17.5 *(3)*	-17.5 *(1)*	-17.3 *(3)*							
Corbula gibba	SF							-20.9 *(1)*			
Corbula laticostata	SF									-25.6 *(2)*	
Corbula sulcata	SF			-16.8 *(1)*							
Glycymeris vovan	SF								-22.1 *(4)*		

Taxa	Trophic mode	Mean δ¹³C per site (number of replicate)									
		1	2	3	4	5	6	7	8	9	10
Mactra glabrata	SF								-19.5 *(3)*	-18.7 *(4)*	
Gregariella petagnae	SF			-17.1 *(1)*							
Modiolus agglutinans	SF					-21.4 *(1)*		-20.6 *(2)*	-20.4 *(3)*		
Modiolus barbatus	SF	-17.5 *(2)*									
Modiolus lutat	SF					-21.1 *(1)*					
Myoforceps aristatus	SF	-17.5 *(3)*	-17.3 *(1)*								
Ostrea sp.	SF	-18.2 *(2)*									
Ostrea stentina	SF			-17.8 *(4)*							
Phaxas pellucidus	SF						-18.5 *(2)*				
Gari fervensis	SF				-17.9 *(1)*	-20.3 *(1)*					
Solemya togata*	SF + SOB										-30.5 *(2)*
Macoma cumana	IF						-18.4 *(3)*		-18.8 *(3)*	-18.7 *(1)*	
Tellina sp.	IF				-16.7 *(1)*		-18.1 *(3)*			-14.9 *(2)*	-14.0 *(1)*
Diplodonta circularis	SF						-19.5 *(3)*				-19.5 *(2)*
Lepidocardia floridella	SF				-18.1 *(3)*	-21.1 *(3)*		-20.5 *(4)*		-18.1 *(3)*	
Veneridae sp. 1	SF				-17.9 *(3)*						
Veneridae sp. 2	SF									-18.7 *(1)*	
Veneridae sp. 3	SF						-19.4 *(1)*	-19.9 *(3)*			
Venerupis dura	SF									-18.6 *(1)*	
Venus verrucosa	SF		-16.7 *(3)*		-18.2 *(1)*						
Cephalopoda											
Octopus vulgaris	P	-14.9 *(5)*									
Gastropoda											
Calyptraea sinensis	SF				-17.2 *(2)*	-20.7 *(2)*					
Crepidula porcellana	SF	-17.2 *(2)*	-17.0 *(2)*		-17.8 *(3)*	-20.7 *(2)*		-20.3 *(3)*			
Persicula blanda	P			-14.1 *(1)*						-11.9 *(1)*	
Persicula cingulata	P				-16.8 *(3)*						
Glabella faba	P									-10.3 *(1)*	
Margina glabella	P			-14.1 *(1)*							
Margina limbata	P		-13.2 *(1)*								
Pugilina morio	P										-17.0 *(5)*
Murex sp.	P					-17.8 *(3)*					
Nassarius miga	P				-15.9 *(1)*	-19.1 *(1)*					
Natica fulminea	P		-15.3 *(1)*		-17.9 *(4)*	-17.5 *(3)*		-20.2 *(3)*	-19.4 *(1)*	-18.7 *(1)*	-14.8 *(1)*
Agaronia acuminata	P									-17.3 *(1)*	
Hastula lepida	P				-17.0 *(1)*						
Gibbula sp.	Gr		-14.3 *(1)*								
Clavatula muricata	P							-16.8 *(1)*	-16.6 *(1)*		
Mesalia opalina	SF			-16.0 *(2)*							
Cymbium cucumis	P			-12.7 *(2)*							
Cymbium spp.	P										-14.8 *(5)*

Taxa	Trophic mode	Mean δ^{13}C per site (number of replicate)									
		1	2	3	4	5	6	7	8	9	10
Scaphopoda											
Dentalium senegalense	P		-13.9 *(1)*		-15.6 *(4)*					-13.1 *(1)*	
Fustiaria maltzani	P				-15.9 *(3)*						
Polychaeta											
Capitellidae sp.	SSDF										-12.2 *(4)*
Eunice vittata	P				-17.5 *(1)*	-17.1 *(3)*		-18.7 *(1)*			
Glycera unicornis	P						-18.1 *(3)*				
Glyceridae sp.	P										-13.4 *(1)*
Goniada multidentata	P						-19.4 *(3)*				
Syllidia sp.	P						-18.1 *(1)*				
Lumbrineris sp.	P						-20.7 *(1)*			-14.2 *(1)*	
Euclymene lumbricoides	SSDF	-13.8 *(2)*									
Euclymene oerstedi	SSDF	-14.2 *(1)*									-13.4 *(3)*
Diopatra cuprea	P	-15.8 *(2)*									
Diopatra neapolitana	P				-16.9 *(1)*	-17.2 *(3)*					
Scoloplos madagascariensis	P				-17.9 *(1)*						
Hypsocomus phaeotaenia	SF			-16.9 *(1)*							
Serpulidae sp.	SF	-16.2 *(1)*									
Sthenelais boa	P						-18.0 *(1)*	-18.0 *(1)*			
Sipunculida	DF	-15.7 *(3)*									
Crustacea											
Clibanarius sp.	P							-17.4 *(3)*			
Dardanus sp.	P			-15.0 *(3)*							
Diogenes sp.	P								-18.4 *(3)*		
Uca tangeri	DF										-9.4 *(6)*
Pagurus sp.	P			-16.9 *(1)*							
Panulirus regius	P	-14.3 *(5)*									
Echinodermata											
Holothuroidea sp. 1	?					-20.7 *(6)*					
Holothuroidea sp. 2	?	-13.0 *(3)*									
Ophiuroidea sp. 1	?										-11.2 *(4)*
Tunicata											
Tunicata sp.1	SF					-21.1 *(3)*					
Tunicata sp.2	SF					-22.4 *(2)*					

Supplement 4: Figure

Mean $\delta^{13}C$ values ($\pm$ SD when n > 2) obtained for benthic secondary consumer invertebrates (omnivorous, scavengers, and predators) at 10 sampling sites. For a given sampling site, each point represents a single species. An asterisk (*) indicates two different species with very similar mean $\delta^{13}C$ values. Dotted lines delimit the same three areas as in Fig. 4.
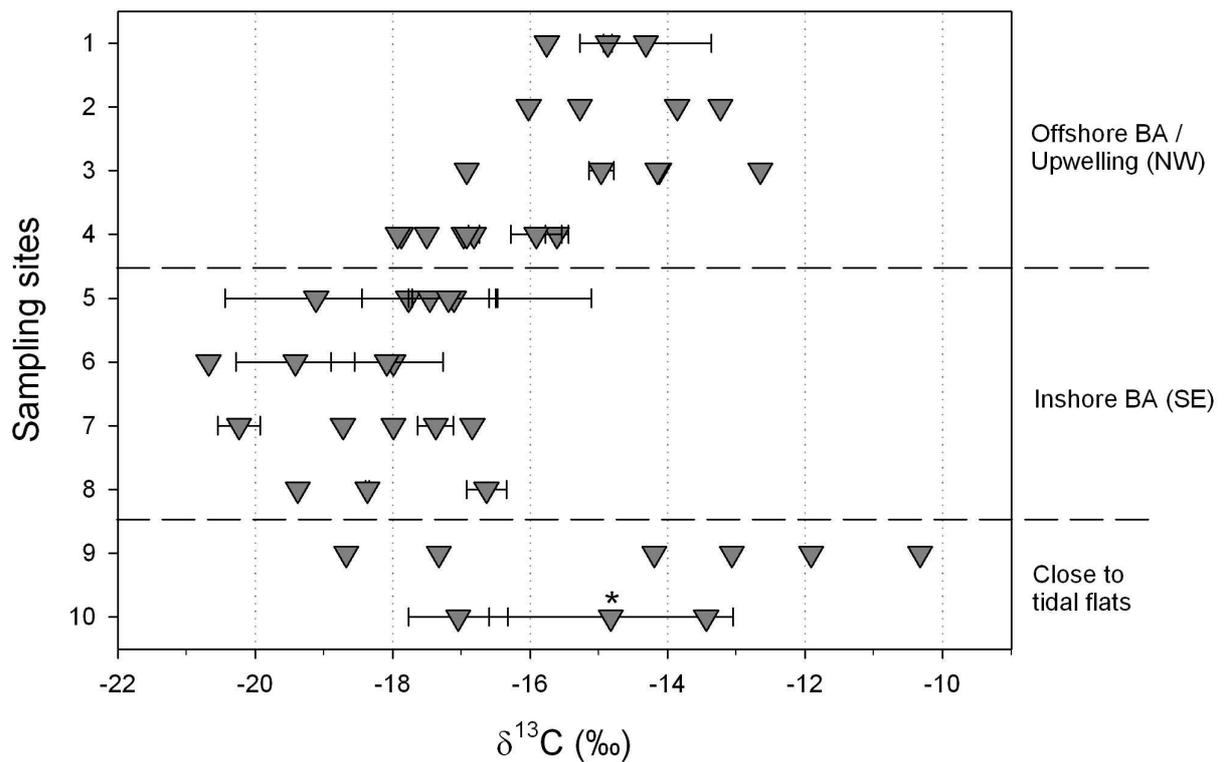
Supplement 5: Table

$\delta^{13}C$ and $\delta^{15}N$ of species of fish sampled during the present study at each fishing site (Mean values ± SD; the number of individuals collected and analyzed is indicated in italics). Trophic modes are zooplanktivorous (Zpl), grazers/deposit feeders (Gr/DF), omnivorous (O), and carnivorous (C).

Order / Species	Trophic mode	Mean sizes (mm)	Nouadhibou $\delta^{13}C$	$\delta^{15}N$	n	Arkeiss $\delta^{13}C$	$\delta^{15}N$	n	Teichott $\delta^{13}C$	$\delta^{15}N$	n
Clupeiformes											
Ethmalosa fimbriata	Zpl	300.0				-17.4 ±	11.8 ±	*1*			
Sardinella aurita	Zpl	261.0	-16.3 ± 0.7	9.3 ± 0.3	*5*						
Sardinella maderensis	Zpl	227.5				-16.8 ± 0.4	10.4 ± 0.7	*4*			
Perciformes											
Alectis alexandrinus	C	476.3				-14.6 ± 2.1	14.6 ± 2.6	*4*			
Campogramma glaycos	C	322.4	-15.9 ± 0.5	13.8 ± 0.4	*5*						
Sarotherodon melanotheron	Gr / DF	286.1							-10.0 ± 3.7	7.7 ± 0.9	*10*
Cynoglossus canariensis	C	437.2	-16.4 ± 0.2	14.6 ± 0.4	*5*						
Drepane africana	C	356.0				-17.9 ± 0.3	17.4 ± 0.1	*5*			
Plectorhinchus mediterraneus	C	346.0	-14.9 ± 0.8	13.4 ± 0.2	*5*						
Pomadasys incisus	C	223.6	-14.9 ± 1.1	13.7 ± 0.6	*5*						
Pomadasys jubelini	C	318.0							-12.5 ± 1.9	10.8 ± 1.2	*5*
Pomadasys rogerii	C	355.0							-13.3 ±	11.3 ±	*1*
Dicentrarchus punctatus	C	303.8	-14.6 ± 0.5	14.3 ± 0.8	*5*						
Liza aurata	Gr / DF	362.4	-13.4 ± 0.7	12.3 ± 0.7	*5*						
Liza grandisquamis	Gr / DF	288.0	-12.2 ± 0.9	14.2 ± 1.4	*5*						
Mugil capurrii	Gr / DF	407.8	-15.4 ± 0.4	12.0 ± 0.8	*5*						
Mugil cephalus	Gr / DF	439.1	-13.1 ± 1.6	12.1 ± 1.9	*10*						
Argyrosomus regius	C	444.2	-14.4 ± 0.1	14.1 ± 0.3	*5*						
Pseudotolithus senegalensis	C	442.0				-15.3 ± 1.2	16.8 ± 1.1	*3*	-11.9 ±	11.5 ±	*2*
Pseudotolithus senegallus	C	600.0							-11.8 ±	13.7 ±	*2*
Umbrina canariensis	C	500.4	-13.7 ± 0.4	14.8 ± 1.5	*5*				-16.0 ± 0.8	13.6 ± 0.5	*5*
Scomberomorus tritor	C	468.6	-17.8 ± 1.1	15.8 ± 0.6	*5*						
Dentex macrophthalmus	C	278.6	-16.0 ± 0.5	12.9 ± 0.3	*5*						
Diplodus sargus	O	242.3	-14.6 ± 1.7	14.1 ± 1.9	*5*				-9.3 ± 0.8	10.8 ± 0.6	*5*
Lithognathus mormyrus	C	241.2	-15.6 ± 0.4	15.6 ± 0.2	*5*						

Order Species	Trophic mode	Mean sizes (mm)	Nouadhibou δ¹³C	δ¹⁵N	n	Arkeiss δ¹³C	δ¹⁵N	n	Teichott δ¹³C	δ¹⁵N	n
Pagellus bellottii	O	236.0	-16.8 ± 0.7	13.0 ± 0.4	5						
Pagrus caeruleostictus	C	328.0	-15.0 ± 0.3	13.1 ± 0.2	5						
Sparus auratus	C	275.6	-15.4 ± 2.6	12.0 ± 1.7	5						
Spondyliosoma cantharus	O	224.4	-15.5 ± 0.9	13.0 ± 0.7	5						
Pleuronectiformes											
Psettodes belcheri	C	485.6	-16.5 ± 0.2	16.8 ± 0.6	5	-16.9 ±	17.0 ±	1			
Psettodes bennettii	C	420.8				-16.9 ± 0.2	17.3 ± 0.1	4	-11.3 ± 1.0	9.8 ± 0.1	5
Solea senegalensis	C	344.8							-11.5 ± 1.4	8.6 ± 0.8	5
Synaptura lusitanica	C	286.5	-15.0 ± 0.3	14.1 ± 0.4	5				-13.6 ±	8.2 ±	1
Siluriformes											
Arius latiscutatus	O	515.0				-12.2 ± 2.1	12.8 ± 1.6	5	-11.9 ± 1.7	11.7 ± 0.7	5
Arius parkii	O	440.9				-14.0 ± 0.1	13.9 ± 0.3	5	-12.9 ± 2.6	11.9 ± 2.7	5
Tetraodontiformes											
Ephippion guttifer	C	462.0							-12.3 ±	8.9 ±	2
Carcharhiniformes											
Carcharhinus obscurus	C	2120.0				-13.0 ±	15.9 ±	1			
Rhizoprionodon acutus	C	942.0				-14.4 ± 0.2	15.9 ± 0.2	5			
Paragaleus pectoralis	C	940.0				-14.0 ±	13.4 ±	1			
Sphyrna lewini	C	763.4				-16.2 ± 0.6	16.9 ± 0.8	5			
Rajiformes											
Gymnura altavela	C	525.0				-15.9 ±	17.2 ±	2			
Pteromylaeus bovinus	C	540.0				-18.1 ±	14.3 ±	1			
Rhinoptera marginata	C	567.0				-16.5 ± 1.0	13.6 ± 0.2	5			